

INFNCA-TH0208

Transverse single spin asymmetries in Drell-Yan processes

M. Anselmino¹, U. D'Alesio², F. Murgia²

¹ *Dipartimento di Fisica Teorica, Università di Torino and
INFN, Sezione di Torino, Via P. Giuria 1, I-10125 Torino, Italy*

² *INFN, Sezione di Cagliari and Dipartimento di Fisica, Università di Cagliari,
C.P. 170, I-09042 Monserrato (CA), Italy*

Abstract

Recently, it has been shown, contrary to previous beliefs, that the \mathbf{k}_\perp distribution of quarks in a transversely polarized proton can be asymmetric. This “Sivers effect” had already been used to explain transverse single spin asymmetries (SSA) observed in inclusive pion production, $p^\uparrow p \rightarrow \pi X$ and $\bar{p}^\uparrow p \rightarrow \pi X$. In such channels, however, other mechanisms, like the “Collins effect” (a \mathbf{k}_\perp asymmetric fragmentation of a transversely polarized quark into pions), may generate SSA. The Sivers asymmetry is used here to compute SSA in Drell-Yan processes; in this case, by considering the differential cross-section in the lepton-pair invariant mass, rapidity and transverse momentum, other mechanisms which may originate SSA cannot contribute. Estimates for RHIC experiments are given.

1. Introduction

Single spin asymmetries in high energy inclusive processes are a unique testing ground for QCD; they cannot originate from the simple spin pQCD dynamics – dominated by helicity conservation – but need some non perturbative chiral-symmetry breaking in the large distance physics. Experiments are rich of puzzling single spin results and more are expected to come; new theoretical ideas and models have just appeared in the literature and a good understanding seems to emerge.

Among the best known transverse single spin asymmetries (SSA) let us mention:

- the old problem of the large polarization of Λ 's and other hyperons produced in the scattering of unpolarized nucleons, $p N \rightarrow \Lambda^\uparrow X$ [1];
- the large asymmetry

$$A_N = \frac{d\sigma^\uparrow - d\sigma^\downarrow}{d\sigma^\uparrow + d\sigma^\downarrow} \quad (1)$$

observed for pion inclusive production, in $p^\uparrow p \rightarrow \pi X$ and $\bar{p}^\uparrow p \rightarrow \pi X$ processes [2];

- the similar azimuthal asymmetry observed in semi-inclusive DIS processes, $\ell p^\uparrow \rightarrow \ell \pi X$ [3].

All of these cannot be related to the elementary dynamics, but rather to non perturbative aspects of the nucleon and hadron structures.

Among the several attempts [4] to explain the data within QCD dynamics we focus here on a phenomenological approach based on the generalization of the factorization theorem with the inclusion of parton intrinsic motion \mathbf{k}_\perp inside a nucleon and of hadrons relatively to the fragmenting parton. The cross-section for a generic process $A B \rightarrow C X$ then reads:

$$d\sigma = \sum_{a,b,c} \hat{f}_{a/A}(x_a, \mathbf{k}_{\perp a}) \otimes \hat{f}_{b/B}(x_b, \mathbf{k}_{\perp b}) \otimes \hat{\sigma}^{ab \rightarrow c \dots}(x_a, x_b, \mathbf{k}_{\perp a}, \mathbf{k}_{\perp b}) \otimes \hat{D}_{C/c}(z, \mathbf{k}_{\perp C}) \quad (2)$$

where the \hat{f} 's are the \mathbf{k}_\perp dependent parton distributions and the \hat{D} 's the \mathbf{k}_\perp dependent fragmentation functions.

The above QCD factorization theorem – with unintegrated \mathbf{k}_\perp dependent distribution and fragmentation functions – has never been formally proven in general [5], but only for the Drell-Yan process (which is the issue of this paper) and for the two-particle inclusive cross-section in e^+e^- annihilation (somehow a time-reversed Drell-Yan process) [6]. However, Eq. (2) has been widely used in the literature, starting from the pioneering work of Feynman, Field and Fox [7]. Actually, several papers have recently shown that intrinsic \mathbf{k}_\perp 's are indeed necessary in order to be able to explain, within pQCD and the factorization scheme, data on large p_T production of pions and photons [8]; without them the theoretical (collinear) computations would give results in some cases much smaller (up to a factor 100) than experiments.

When dealing with polarized processes the introduction of \mathbf{k}_\perp dependences opens up the way to many possible spin effects; these can be summarized, at leading twist, by new polarized distribution functions,

$$\Delta^N f_{q/p^\uparrow} \equiv \hat{f}_{q/p^\uparrow}(x, \mathbf{k}_\perp) - \hat{f}_{q/p^\downarrow}(x, \mathbf{k}_\perp) = \hat{f}_{q/p^\uparrow}(x, \mathbf{k}_\perp) - \hat{f}_{q/p^\uparrow}(x, -\mathbf{k}_\perp) \quad (3)$$

$$\Delta^N f_{q^\uparrow/p} \equiv \hat{f}_{q^\uparrow/p}(x, \mathbf{k}_\perp) - \hat{f}_{q^\downarrow/p}(x, \mathbf{k}_\perp) = \hat{f}_{q^\uparrow/p}(x, \mathbf{k}_\perp) - \hat{f}_{q^\uparrow/p}(x, -\mathbf{k}_\perp) \quad (4)$$

and new polarized fragmentation functions,

$$\Delta^N D_{h/q^\uparrow} \equiv \hat{D}_{h/q^\uparrow}(z, \mathbf{k}_\perp) - \hat{D}_{h/q^\downarrow}(z, \mathbf{k}_\perp) = \hat{D}_{h/q^\uparrow}(z, \mathbf{k}_\perp) - \hat{D}_{h/q^\uparrow}(z, -\mathbf{k}_\perp) \quad (5)$$

$$\Delta^N D_{h^\uparrow/q} \equiv \hat{D}_{h^\uparrow/q}(z, \mathbf{k}_\perp) - \hat{D}_{h^\downarrow/q}(z, \mathbf{k}_\perp) = \hat{D}_{h^\uparrow/q}(z, \mathbf{k}_\perp) - \hat{D}_{h^\uparrow/q}(z, -\mathbf{k}_\perp) \quad (6)$$

which have a clear meaning if one pays attention to the arrows denoting the polarized particles. All the above functions vanish when $k_\perp = 0$ and are naïvely T -odd. The ones in Eqs. (4) and (5), when written in the helicity basis, relate quarks of different helicities and are chiral-odd, while the other two are chiral-even.

Similar functions have been introduced in the literature with different notations: in particular there is a direct correspondence [9] between the above functions and the ones denoted, respectively, by: f_{1T}^\perp [10], h_1^\perp [11], H_1^\perp and D_{1T}^\perp [10, 12].

In the recent comprehensive review paper on transverse quark polarization [13] the following notations are used: $\Delta^N f_{q/p^\uparrow} \equiv \Delta_0^T f$, $\Delta^N f_{q^\uparrow/p} \equiv \Delta_T^0 f$ and $\Delta^N D_{h/q^\uparrow} \equiv 2\Delta_T^0 D_{h/q}$.

The fragmentation in Eq. (5) is the Collins function [5], while the distribution in Eq. (3) was first introduced by Sivers [14].

Some of the above functions have been used for a phenomenological description of the observed SSA. Both Sivers [15] and Collins [16, 17] functions can explain the E704 data on A_N [2]: the Collins asymmetry might have been indirectly observed in HERMES data [3] and the polarizing fragmentation functions (6) can describe [18] the Λ polarization data [1].

Despite its successful phenomenology, the Sivers function was always a matter of discussions and its very existence rather controversial; in fact in Ref. [5] a proof of its vanishing was given, based on time-reversal invariance. Ways out based on initial state interactions [15] or non standard time-reversal properties [19] were discussed, but the situation remained uncertain and further phenomenology was performed making use of the Collins function only [16]. A similar criticism applied to the function in Eq. (4).

Very recently a series of papers have resurrected Sivers asymmetry in its full rights. First, in Ref. [20], a quark-diquark model calculation including final state effects has given an explanation of the HERMES azimuthal asymmetry different from the one originating from Collins function. As a consequence, Collins recognised [21] that such a new mechanism is compatible with factorization and is due to the Sivers asymmetry (3); re-examining his original proof of the vanishing of $\Delta^N f_{q/p^\uparrow}$ he finds it to be invalidated by the path-ordered exponential of the gluon field in the

operator definition of parton densities. The authors of Ref. [22] have confirmed the model results of [20]; a second paper by Brodsky, Hwang and Schmidt [23], along the same lines of the first one, shows that initial state interactions give rise to SSA in Drell-Yan processes.

Some issues concerning factorizability and universality of these effects are still open to debate; however, we feel now confident to use Sivvers effects – and equally all functions in Eqs. (3)-(6) – in SSA phenomenology. The natural process to test the Sivvers asymmetry is Drell-Yan: in such a case there cannot be any effect in fragmentation processes and, by suitably integrating over some final configurations, also possible effects from transversely polarized quarks in an unpolarized proton, Eq. (4), do not contribute. SSA in Drell-Yan processes are particularly important now, as ongoing or imminent experiments at RHIC will be able to measure them.

The paper is organized as follows: in Section 2 we present the formalism necessary to discuss single spin asymmetries in Drell-Yan processes, taking into account the transverse motion of partons in nucleons. Some simple analytical formulae are also derived, assuming simplified functional k_\perp dependences. In Section 3 we give some numerical estimates for SSA at RHIC, while comments and conclusions are gathered in Section 4.

2. SSA in Drell-Yan processes, formalism

Let us consider a Drell-Yan process, that is the production of $\ell^+\ell^-$ pairs in the collision of two hadrons A and B ; there is no need of any fragmentation function and Eq. (2) reads:

$$d\sigma = \sum_{ab} \int [dx_a d^2\mathbf{k}_{\perp a} dx_b d^2\mathbf{k}_{\perp b}] \hat{f}_{a/A}(x_a, \mathbf{k}_{\perp a}) \hat{f}_{b/B}(x_b, \mathbf{k}_{\perp b}) d\hat{\sigma}^{ab \rightarrow \ell^+\ell^-} \quad (7)$$

and, from the Sivvers asymmetry of Eq. (3), the difference between the single transverse spin dependent cross-sections $d\sigma^\uparrow$ for $A^\uparrow B \rightarrow \ell^+\ell^- X$ and $d\sigma^\downarrow$ for $A^\downarrow B \rightarrow \ell^+\ell^- X$ is

$$d\sigma^\uparrow - d\sigma^\downarrow = \sum_{ab} \int [dx_a d^2\mathbf{k}_{\perp a} dx_b d^2\mathbf{k}_{\perp b}] \Delta^N f_{a/A^\uparrow}(x_a, \mathbf{k}_{\perp a}) \hat{f}_{b/B}(x_b, \mathbf{k}_{\perp b}) d\hat{\sigma}^{ab \rightarrow \ell^+\ell^-}. \quad (8)$$

The elementary cross-section $d\hat{\sigma}$ for the process $a(p_a) b(p_b) \rightarrow \ell^+(p_+) \ell^-(p_-)$ is given by:

$$d\hat{\sigma} = \frac{1}{2\hat{s}} \frac{d^3p_+}{2E_+} \frac{d^3p_-}{2E_-} \frac{1}{(2\pi)^2} \delta^4(p_a + p_b - p_+ - p_-) \overline{|M_{ab \rightarrow \ell^+\ell^-}|^2}. \quad (9)$$

We consider the differential cross-section in the variables

$$\hat{s} \equiv M^2 = (p_a + p_b)^2 \equiv q^2 \quad y = \frac{1}{2} \ln \frac{q_0 + q_L}{q_0 - q_L} \quad \mathbf{q}_T, \quad (10)$$

that is the squared invariant mass, the rapidity and the transverse momentum of the lepton pair; q_0 , \mathbf{q}_T and q_L are respectively the energy, transverse and longitudinal components, in the A - B center of mass frame, of the four-vector $q = p_a + p_b = p_+ + p_-$.

Using the relations:

$$\frac{d^3 p_-}{2E_-} = d^4 p_- \delta(p_-^2) \quad p_- = q - p_+ \quad dM^2 dy = 2 dq_0 dq_L, \quad (11)$$

Eq. (8) can be written as

$$\begin{aligned} \frac{d^4 \sigma^\uparrow}{dy dM^2 d^2 \mathbf{q}_T} - \frac{d^4 \sigma^\downarrow}{dy dM^2 d^2 \mathbf{q}_T} &= \frac{1}{2} \sum_{ab} \int [dx_a d^2 \mathbf{k}_{\perp a} dx_b d^2 \mathbf{k}_{\perp b}] \\ \Delta^N f_{a/A^\uparrow}(x_a, \mathbf{k}_{\perp a}) \hat{f}_{b/B}(x_b, \mathbf{k}_{\perp b}) \delta^4(p_a + p_b - q) \hat{\sigma}_0^{ab} \end{aligned} \quad (12)$$

where $\hat{\sigma}_0^{ab}$ is the total cross-section for the $ab \rightarrow \ell^+ \ell^-$ process:

$$\hat{\sigma}_0^{ab} = \int \frac{d^3 p_+}{2E_+} \frac{1}{(2\pi)^2} \frac{1}{2M^2} \delta((q - p_+)^2) \overline{|M_{ab \rightarrow \ell^+ \ell^-}(p_+, q)|^2}. \quad (13)$$

Analogously

$$\begin{aligned} \frac{d^4 \sigma^\uparrow}{dy dM^2 d^2 \mathbf{q}_T} + \frac{d^4 \sigma^\downarrow}{dy dM^2 d^2 \mathbf{q}_T} &= \sum_{ab} \int [dx_a d^2 \mathbf{k}_{\perp a} dx_b d^2 \mathbf{k}_{\perp b}] \\ \hat{f}_{a/A}(x_a, \mathbf{k}_{\perp a}) \hat{f}_{b/B}(x_b, \mathbf{k}_{\perp b}) \delta^4(p_a + p_b - q) \hat{\sigma}_0^{ab} \end{aligned} \quad (14)$$

which is twice the unpolarized cross-section.

For Drell-Yan processes the dominating electromagnetic elementary interaction is $q\bar{q} \rightarrow \gamma^* \rightarrow \ell^+ \ell^-$, so that $a, b = q, \bar{q}$ with $q = u, \bar{u}, d, \bar{d}, s, \bar{s}$ and:

$$\hat{\sigma}_0^{q\bar{q}} = \frac{4\pi\alpha^2 e_q^2}{9M^2}. \quad (15)$$

Eqs. (12) and (14) allow to compute a single spin asymmetry A_N , Eq. (1), for Drell-Yan processes and for differential cross-sections measuring the lepton pair invariant mass M , rapidity y and transverse momentum \mathbf{q}_T ; notice that we do not look at the angular distribution of the lepton pair production plane, which is integrated over.

Let us now fix in more details our kinematical configuration. We take the hadron A as moving along the positive z -axis, in the A - B c.m. frame and measure the transverse polarization of hadron A , \mathbf{P}_A , along the y -axis, as shown in Fig. 1. Neglecting masses, the four-momenta of hadrons and partons are:

$$p_A = \frac{\sqrt{s}}{2} (1, 0, 0, 1) \quad p_B = \frac{\sqrt{s}}{2} (1, 0, 0, -1) \quad (16)$$

$$p_a = x_a \frac{\sqrt{s}}{2} \left(1 + \frac{k_{\perp a}^2}{x_a^2 s}, \frac{2\mathbf{k}_{\perp a}}{x_a \sqrt{s}}, 1 - \frac{k_{\perp a}^2}{x_a^2 s} \right) \quad (17)$$

$$p_b = x_b \frac{\sqrt{s}}{2} \left(1 + \frac{k_{\perp b}^2}{x_b^2 s}, \frac{2\mathbf{k}_{\perp b}}{x_b \sqrt{s}}, -1 + \frac{k_{\perp b}^2}{x_b^2 s} \right) \quad (18)$$

with

$$q = p_a + p_b = (q_0, \mathbf{q}_T, q_L) = \left(\sqrt{M^2 + q_T^2} \cosh y, \mathbf{q}_T, \sqrt{M^2 + q_T^2} \sinh y \right), \quad (19)$$

where the lepton pair rapidity y and invariant mass M are defined in Eq. (10).

The four-momentum conservation δ function of Eqs. (12) and (14) contains the factors:

$$\begin{aligned} & \frac{1}{2} \delta(E_a + E_b - q_0) \delta(p_{za} + p_{zb} - q_L) = \\ & \frac{1}{2} \delta \left((x_a + x_b) \frac{\sqrt{s}}{2} + \left[\frac{k_{\perp a}^2}{x_a s} + \frac{k_{\perp b}^2}{x_b s} \right] \frac{\sqrt{s}}{2} - q_0 \right) \times \\ & \delta \left((x_a - x_b) \frac{\sqrt{s}}{2} - \left[\frac{k_{\perp a}^2}{x_a s} - \frac{k_{\perp b}^2}{x_b s} \right] \frac{\sqrt{s}}{2} - q_L \right). \end{aligned} \quad (20)$$

We shall consider kinematical regions such that:

$$q_T^2 \ll M^2 \quad k_{\perp a, b}^2 \simeq q_T^2, \quad (21)$$

where Eq. (20) simplifies into the usual collinear condition:

$$\frac{1}{2} \delta(E_a + E_b - q_0) \delta(p_{za} + p_{zb} - q_L) = \frac{1}{s} \delta \left(x_a - \frac{M}{\sqrt{s}} e^y \right) \delta \left(x_b - \frac{M}{\sqrt{s}} e^{-y} \right). \quad (22)$$

In such a region [$q_T^2 \ll M^2$, $q_T \simeq k_{\perp}$] then one has

$$A_N = \frac{\sum_q e_q^2 \int d^2 \mathbf{k}_{\perp q} d^2 \mathbf{k}_{\perp \bar{q}} \delta^2(\mathbf{k}_{\perp q} + \mathbf{k}_{\perp \bar{q}} - \mathbf{q}_T) \Delta^N f_{q/A^\dagger}(x_q, \mathbf{k}_{\perp q}) \hat{f}_{\bar{q}/B}(x_{\bar{q}}, \mathbf{k}_{\perp \bar{q}})}{2 \sum_q e_q^2 \int d^2 \mathbf{k}_{\perp q} d^2 \mathbf{k}_{\perp \bar{q}} \delta^2(\mathbf{k}_{\perp q} + \mathbf{k}_{\perp \bar{q}} - \mathbf{q}_T) \hat{f}_{q/A}(x_q, \mathbf{k}_{\perp q}) \hat{f}_{\bar{q}/B}(x_{\bar{q}}, \mathbf{k}_{\perp \bar{q}})} \quad (23)$$

with x_q and $x_{\bar{q}}$ fixed by Eq. (22) with $a, b = q, \bar{q}$ and $q = u, \bar{u}, d, \bar{d}, s, \bar{s}$.

2.1 Other mechanisms for SSA in Drell-Yan processes

Before discussing further Eq. (23), let us comment on other possible origins of SSA. Let us consider first the SSA generated by the distribution function in Eq. (4), as compared with Sivers mechanism, Eq. (3), which we are considering here. The main point is that, as we have seen, Eq. (3) gives a contribution to A_N of the type:

$$\sum_q \Delta^N f_{q/A^\dagger}(x_a, \mathbf{k}_{\perp a}) \otimes \hat{f}_{\bar{q}/B}(x_b, \mathbf{k}_{\perp b}) \otimes d\hat{\sigma}^{q\bar{q} \rightarrow \ell^+ \ell^-} \quad (24)$$

where $d\hat{\sigma}$ is the elementary unpolarized cross-section, while Eq. (4) leads to a contribution of the kind [11]

$$\sum_q h_{1q}(x_a, \mathbf{k}_{\perp a}) \otimes \Delta^N f_{\bar{q}^\dagger/B}(x_b, \mathbf{k}_{\perp b}) \otimes d\Delta\hat{\sigma}^{q\bar{q} \rightarrow \ell^+ \ell^-} \quad (25)$$

where h_{1q} is the transversity of quark q (inside hadron A) and $d\Delta\hat{\sigma}$ is the double transverse spin asymmetry $d\hat{\sigma}^{\uparrow\uparrow} - d\hat{\sigma}^{\uparrow\downarrow}$. Such an elementary asymmetry has a $\cos 2\phi$ dependence [11, 24], where ϕ is the angle between the transverse polarization direction and the normal to the $\ell^+\ell^-$ plane; when integrating over all final angular distributions of the $\ell^+\ell^-$ pair – as we do by looking only at variables (10) – the contribution of Eq. (25) vanishes.

There exist in the literature other mechanisms to generate SSA in Drell-Yan processes [25, 26, 27, 28], based on higher twist quark-gluon correlation functions in a generalized pQCD factorization theorem [29]. All of them lead to expressions of A_N depending on the angles between the polarization direction and the final lepton pair plane [30], which require observation of these angles to be detected and vanish upon integration.

In the model of Ref. [31] a SSA for the differential cross-section (14) is computed: in that model a non vanishing asymmetry is achieved by introducing orbital angular momentum and surface effects in the distribution of valence quarks, resulting in somewhat *ad hoc* correlations between their polarization and \mathbf{k}_\perp distribution. It might be that the mechanism is somehow related to the Sivers effect, although the issue should be further investigated.

In Refs. [20] and [23] – which are meant to be and provide important pedagogical examples of SSA – the processes considered are somehow academic and related by crossing. They are respectively $\gamma^* p^\uparrow \rightarrow q(q\bar{q})_0$ and $\bar{q} p^\uparrow \rightarrow \gamma^*(q\bar{q})_0$ where $(q\bar{q})_0$ is a spectator scalar diquark. The SSA obtained in these two cases turn out to be opposite, as predicted by Collins [21].

2.2 A simple analytical model

In order to give numerical estimates in the next Section, we introduce here a simple model for the Sivers asymmetry (3), and for the unpolarized distributions, which is similar to the one introduced for the polarizing fragmentation function in Ref. [32] and has the advantage of giving analytically integrable expressions for A_N . Such a model shows explicitly how the asymmetry originates and depends on M , y and \mathbf{q}_T .

Let us start from the most general expression for the number density of quarks q , inside a proton with transverse polarization \mathbf{P} and three-momentum \mathbf{p} ; the quark has a transverse momentum \mathbf{k}_\perp and its polarization is not observed. One has

$$\hat{f}_{q/p^\uparrow}(x, \mathbf{k}_\perp) = \hat{f}_{q/p}(x, k_\perp) + \frac{1}{2} \Delta^N f_{q/p^\uparrow}(x, k_\perp) \hat{\mathbf{P}} \cdot \hat{\mathbf{p}} \times \hat{\mathbf{k}}_\perp, \quad (26)$$

consistently with Eq. (3)

$$\hat{f}_{q/p^\uparrow}(x, \mathbf{k}_\perp) + \hat{f}_{q/p^\downarrow}(x, \mathbf{k}_\perp) = 2 \hat{f}_{q/p}(x, \mathbf{k}_\perp) = 2 \hat{f}_{q/p}(x, k_\perp) \quad (27)$$

$$\hat{f}_{q/p^\uparrow}(x, \mathbf{k}_\perp) - \hat{f}_{q/p^\downarrow}(x, \mathbf{k}_\perp) = \Delta^N f_{q/p^\uparrow}(x, \mathbf{k}_\perp) = \Delta^N f_{q/p^\uparrow}(x, k_\perp) \hat{\mathbf{P}} \cdot \hat{\mathbf{p}} \times \hat{\mathbf{k}}_\perp. \quad (28)$$

With the configuration of Fig. 1 one simply has $\hat{\mathbf{P}} \cdot \hat{\mathbf{p}} \times \hat{\mathbf{k}}_\perp = (\hat{\mathbf{k}}_\perp)_x = \cos \phi_{k_\perp}$.

The Siverts function $\Delta^N f_{q/p^\dagger}(x, k_\perp)$ must obey the positivity bound:

$$\frac{|\Delta^N f_{q/p^\dagger}(x, k_\perp)|}{2 \hat{f}_{q/p}(x, k_\perp)} \leq 1 \quad \forall x, k_\perp. \quad (29)$$

We consider simple factorized and Gaussian forms:

$$\hat{f}_{q/p}(x, k_\perp) = f_{q/p}(x) g(k_\perp) = f_{q/p}(x) \frac{\beta^2}{\pi} e^{-\beta^2 k_\perp^2}, \quad (30)$$

$$\Delta^N f_{q/p^\dagger}(x, k_\perp) = \Delta^N f_{q/p^\dagger}(x) h(k_\perp). \quad (31)$$

Notice that β can depend on x ; we have assumed the same k_\perp dependence for all flavours, as intrinsic \mathbf{k}_\perp of quarks originates via confinement and gluon emissions, which should be flavour independent processes. Notice also that $\beta^2 = 1/\langle k_\perp^2 \rangle$ and that $\int d^2 \mathbf{k}_\perp \hat{f}_{q/p}(x, k_\perp) = f_{q/p}(x)$.

In order to obviously satisfy the bound (29) we write

$$\Delta^N f_{q/p^\dagger}(x) = 2 \mathcal{N}_q(x) f_{q/p}(x) \quad (32)$$

$$h(k_\perp) = \mathcal{H}(k_\perp) g(k_\perp). \quad (33)$$

so that Eq. (29) simply becomes

$$|\mathcal{N}_q(x) \mathcal{H}(k_\perp)| \leq 1 \quad \forall x, k_\perp. \quad (34)$$

We actually impose \mathcal{N} and \mathcal{H} to be separately smaller than 1 in magnitude, by choosing simple analytical functional forms and dividing each of them by its maximum value:

$$\mathcal{N}_q(x) = N_q x^{a_q} (1-x)^{b_q} \frac{(a_q + b_q)^{(a_q + b_q)}}{a_q^{a_q} b_q^{b_q}}, \quad |N_q| \leq 1 \quad (35)$$

$$\mathcal{H}(k_\perp) = \sqrt{2e(\alpha^2 - \beta^2)} k_\perp \exp \left[-(\alpha^2 - \beta^2) k_\perp^2 \right], \quad \alpha > \beta. \quad (36)$$

Eqs. (30)-(33) and (36) imply:

$$\Delta^N f_{q/p^\dagger}(x, k_\perp) = 2 \mathcal{N}_q(x) f_{q/p}(x) \frac{\beta^2}{\pi} \sqrt{2e(\alpha^2 - \beta^2)} k_\perp e^{-\alpha^2 k_\perp^2}. \quad (37)$$

Inserting the above choice of $\Delta^N f(x, \mathbf{k}_\perp)$ and $\hat{f}(x, \mathbf{k}_\perp)$ into Eq. (23) one can perform analytical integrations. The numerator of Eq. (23) results as:

$$\begin{aligned} N(A_N) &= \frac{1}{\pi} \frac{\beta^3 \bar{\beta}^4}{(\alpha^2 + \beta^2)^2} \left(2e \frac{\alpha^2 - \beta^2}{\beta^2} \right)^{1/2} (\mathbf{q}_T)_x \exp \left[-\frac{\alpha^2 \bar{\beta}^2}{\alpha^2 + \beta^2} q_T^2 \right] \\ &\times \sum_q e_q^2 \Delta^N f_{q/p^\dagger}(x_q) \hat{f}_{\bar{q}/p}(x_{\bar{q}}) \end{aligned} \quad (38)$$

where $\alpha = \alpha(x_q)$, $\beta = \beta(x_q)$, $\bar{\beta} = \beta(x_{\bar{q}})$ with $x_q = M e^y / \sqrt{s}$, $x_{\bar{q}} = M e^{-y} / \sqrt{s}$. The denominator is

$$D(A_N) = \frac{1}{\pi} \frac{\beta^2 \bar{\beta}^2}{\beta^2 + \bar{\beta}^2} \exp \left[-\frac{\beta^2 \bar{\beta}^2}{\beta^2 + \bar{\beta}^2} q_T^2 \right] 2 \sum_q e_q^2 f_{q/p}(x_q) f_{\bar{q}/p}(x_{\bar{q}}), \quad (39)$$

where again β stands for $\beta(x_q)$ and $\bar{\beta}$ for $\beta(x_{\bar{q}})$.

The asymmetry (23) in this simple case reads:

$$\begin{aligned} A_N(M, y, \mathbf{q}_T) &= \beta \bar{\beta}^2 \frac{\beta^2 + \bar{\beta}^2}{(\alpha^2 + \beta^2)^2} \left(2 e \frac{\alpha^2 - \beta^2}{\beta^2} \right)^{1/2} \\ &\times (\mathbf{q}_T)_x \exp \left[-\left(\frac{\alpha^2}{\alpha^2 + \bar{\beta}^2} - \frac{\beta^2}{\beta^2 + \bar{\beta}^2} \right) \bar{\beta}^2 q_T^2 \right] \\ &\times \frac{1}{2} \frac{\sum_q e_q^2 \Delta^N f_{q/p}(x_q) f_{\bar{q}/p}(x_{\bar{q}})}{\sum_q e_q^2 f_{q/p}(x_q) f_{\bar{q}/p}(x_{\bar{q}})}. \end{aligned} \quad (40)$$

For a generic configuration, different from the one of Fig. 1, one simply replaces $(\mathbf{q}_T)_x$ with $\hat{\mathbf{P}} \cdot \hat{\mathbf{p}} \times \mathbf{q}_T$.

When, as it is often the case in the literature, α and β are taken to be independent of x , Eq. (40) simplifies to:

$$\begin{aligned} A_N(M, y, \mathbf{q}_T) &= \frac{2 \beta^5}{(\alpha^2 + \beta^2)^2} \left(2 e \frac{\alpha^2 - \beta^2}{\beta^2} \right)^{1/2} \\ &\times (\mathbf{q}_T)_x \exp \left[-\left(\frac{\alpha^2}{\alpha^2 + \beta^2} - \frac{1}{2} \right) \beta^2 q_T^2 \right] \\ &\times \frac{1}{2} \frac{\sum_q e_q^2 \Delta^N f_{q/p}(x_q) f_{\bar{q}/p}(x_{\bar{q}})}{\sum_q e_q^2 f_{q/p}(x_q) f_{\bar{q}/p}(x_{\bar{q}})}. \end{aligned} \quad (41)$$

The same simplified expression holds also at $y = 0$, where one has $x_q = x_{\bar{q}} = M/\sqrt{s}$.

3. SSA in Drell-Yan processes, numerical estimates

In this Section we shall present numerical estimates of the SSA for the Drell-Yan process, originating from Sivers effect, in kinematical configurations relevant for RHIC experiments.

We follow the simple analytical model discussed in the previous Section; we need to fix the parameters of the model, that is the functions $\beta(x)$, $\alpha(x)$ and the flavour-dependent coefficients N_q , a_q , b_q appearing respectively in Eqs. (30), (37) and (35). The unpolarized and \mathbf{k}_\perp integrated partonic distributions are chosen among the sets available in the literature; in particular, we adopt the GRV94 set [33].

Some information on β , entering the \mathbf{k}_\perp dependence in the unpolarized parton distributions, can be obtained by considering the available data on the unpolarized

cross-sections for inclusive particle production processes. This not only supplies information on β , but allows a crucial consistency check of our formalism, as it shows whether or not we can reproduce the unpolarized data.

Experimental data are presently available for pion, prompt photon production and for Drell-Yan processes, in different kinematical configurations. As mentioned in the introduction, several papers [8] have studied in details the unpolarized cross-sections for these processes within perturbative QCD at LO and NLO, emphasizing the crucial role of intrinsic transverse momentum.

We have performed an independent attempt of reproducing the available data within the same approach utilized in the calculation of the SSA. Since SSA have been studied at present only at leading order and leading twist, the same level of accuracy has been adopted for the unpolarized cross-sections, keeping in mind that there might be NLO corrections (the so-called K factors) the value of which may vary, depending on the process and on the kinematical configuration considered, approximately between a factor 1 and 3.

Our aim is not to reproduce as accurately as possible the unpolarized cross-sections, as in [8], but rather to show that within the same approach used for the SSA it is possible to reproduce the unpolarized cross-section values, up to an overall factor between 1 and 3, due to NLO corrections, scale-dependences, etc. These corrections should have little effect on the SSA, largely canceling in the ratio of cross-sections.

A full account of the combined study of unpolarized cross-sections and SSA in different processes is outside the scope of this paper, and will be given in a separate forthcoming paper [34]. It suffices to state here that, as a result of this comprehensive analysis, a value of β independent of x , $\beta = 1.25 (\text{GeV}/c)^{-1}$, corresponding to $\sqrt{\langle k_{\perp}^2 \rangle} = 0.8 \text{ GeV}/c$, allows a good description of the unpolarized processes and is appropriate for our scope. This value is in good agreement with the results of the abovementioned papers devoted to unpolarized cross-section calculations [8], and will be adopted in the sequel.

One might argue that the value of β varies with energy and that RHIC works at c.m. energies much larger than most of previous experiments; this could be tested when RHIC data on unpolarized cross-sections will become available and, for the moment, we keep using the value $\beta = 1.25 (\text{GeV}/c)^{-1}$, which corresponds to an already large $\langle k_{\perp} \rangle$ value. We only notice that in our approach changes in β should influence only the dependence of the SSA on $|\mathbf{q}_T|$. In the following, we will show such a dependence by presenting some of our results for $\beta = 0.83 (\text{GeV}/c)^{-1}$, which means $\sqrt{\langle k_{\perp}^2 \rangle} = 1.2 \text{ GeV}/c$.

Adopting a β parameter independent of x and, as we do, of quark flavour, simplifies our analytical expressions as one gets $\bar{\beta} \equiv \beta$, which allows the use of Eq. (41).

As a second step, we must fix the parameter α determining the gaussian shape of the Sivers function, see Eq. (37). Since the positivity bound, Eq. (29), requires $\alpha > \beta$, one can write $\alpha^2 = \beta^2/r$, where r is a numerical parameter in the range (0, 1).

A similar procedure was already followed by us in a previous work on transverse hyperon polarization [32], and an optimal guess for the parameter r was found, $r \simeq 0.7$, value which we also adopt here. The same value allows a good description, using Siverts function, of the E704 data on A_N [2, 34].

The next step is to obtain information on the x -dependent part of the Siverts function, $\Delta^N f_{q/p^\uparrow}(x)$. Indications on the values of the parameters entering Eq. (35) can be obtained by exploiting the data on SSA measured by the E704 experiment [2] for the process $p^\uparrow p \rightarrow \pi X$.

Estimates of the Siverts function from E704 results were already given and used to make predictions for SSA in similar processes in [15]. In those first papers, however, a number of simplifying approximations were adopted which are not kept in the present, more general, analysis. Those assumptions amounted to consider \mathbf{k}_\perp effects only minimally, in places where their neglect would lead to vanishing results; also, no gaussian k_\perp distribution was introduced, but rather a simple δ -like dependence which leads to the effective use of an average k_\perp in a simplified (planar) kinematics.

Although the simplified procedure might be a good approximation for single spin asymmetries, which are ratios of cross-sections, a more general and refined analysis, using full \mathbf{k}_\perp dependences according to Eq. (2), is in progress and a detailed analysis will be presented elsewhere [34]; we only state here that good reproductions of both the cross-sections and the E704 asymmetry are possible and a good set of values for the parameters N_q , a_q and b_q of the Siverts function is:

$$\begin{aligned} N_u &= 0.5 & a_u &= 2.0 & b_u &= 0.3 & , \\ N_d &= -1.0 & a_d &= 1.5 & b_d &= 0.2 & . \end{aligned} \quad (42)$$

Notice that we are assuming that only valence quarks in the proton give a nonvanishing Siverts function.

The above values allow a good description of the E704 data on the SSA in the $p^\uparrow p \rightarrow \pi X$ process [2], assuming that A_N is totally generated by Siverts asymmetric distribution. We use them here in order to estimate A_N for a D-Y process at a much higher energy: we are well aware that this might be a rough extrapolation, as we neglect pQCD evolution, other possible mechanisms, and so on. However, since information on Siverts function is so scarce, even rough estimates of the SSA in Drell-Yan processes are important and useful, and we shall proceed with our program, keeping in mind all these remarks.

One further uncertainty concerns the sign of the asymmetry: as noticed by Collins [21] and checked in Ref. [23], the Siverts asymmetry has opposite signs in Drell-Yan and SIDIS, respectively related to s -channel and t -channel elementary reactions. As in $p-p$ interactions we expect, at large x_F , a dominant contribution from t -channel quark processes, we think that the Siverts function extracted from $p-p$ data should be opposite to that contributing to D-Y processes. Our numerical estimates will then be given with the same parameters as in Eq. (42), *changing the signs of N_u and N_d* . Given these considerations, even a simple comparison of the sign of our estimates with data might be significant.

We have thus completed the choice of parameters of our model, and we are now able to give predictions for the Drell-Yan process, without forgetting all the cautious comments made above.

We only add that a different modelization of the Sivers function, originally proposed by Collins for his function [5] and often adopted in the literature, could be used. This functional form does not allow to perform exact analytical integrations on transverse momentum, and we prefer using the form proposed here. However, we have checked that for consistent choices of the parameters, the two parameterizations give very similar results, since they mainly differ at relatively large transverse momentum, where the gaussian dumping is already effective.

An important point has to be noticed regarding the parameterization of the Sivers function. In order to reproduce the E704 results, it has to have a valence-like behaviour. That is, $\Delta^N f_{q/p^\uparrow}(x)/f_{q/p}(x) \sim x^a$, where $a > 0$, for small x .

This is a very general feature, somehow required by the experimental data, which may have strong effects for the SSA in Drell-Yan processes, leading to tiny values of A_N when the x values explored are relatively small. This prediction and its extent of validity can be tested at RHIC. In what follows, we shall show some estimates for the SSA in realistic kinematical regions:

$$6 \text{ GeV} \leq M \leq 10 \text{ GeV}; \quad -2 \leq y \leq 2. \quad (43)$$

To show the dependence on the range of invariant mass covered, we will consider also the alternative set of kinematical cuts

$$10 \text{ GeV} \leq M \leq 20 \text{ GeV}; \quad -2 \leq y \leq 2. \quad (44)$$

These kinematical regions should be easily explored in RHIC experiments, while assuring that the Drell-Yan process is the dominating contribution to lepton pair production. Notice that with the above cuts the lowest possible value of x reached is around 10^{-3} .

In our simple analytical model, the dependences of A_N on \mathbf{q}_T and $x_q, x_{\bar{q}}$ (or M, y) are completely uncorrelated, and may be treated separately. In fact, assuming $\bar{\beta} \equiv \beta$ and $\alpha^2 = \beta^2/r$, Eq. (40) now reads

$$\begin{aligned} A_N(M, y, \mathbf{q}_T) &= \mathcal{Q}(q_T, \phi_{q_T}) \mathcal{A}(M, y) \\ &= 2 \frac{r^2}{(1+r)^2} \left(2e \frac{1-r}{r} \right)^{1/2} \beta q_T \cos \phi_{q_T} \exp \left[-\frac{1}{2} \frac{1-r}{1+r} \beta^2 q_T^2 \right] \\ &\times \frac{1}{2} \frac{\sum_q e_q^2 \Delta^N f_{q/p^\uparrow}(x_q) f_{\bar{q}/p}(x_{\bar{q}})}{\sum_q e_q^2 f_{q/p}(x_q) f_{\bar{q}/p}(x_{\bar{q}})}. \end{aligned} \quad (45)$$

where ϕ_{q_T} is the azimuthal angle of \mathbf{q}_T , as defined in Fig. 1.

The second line of the above equation, the function $\mathcal{Q}(\mathbf{q}_T)$, describes the \mathbf{q}_T dependence of the asymmetry, which turns out to be very simple and directly related

to the \mathbf{k}_\perp behaviour of the Sivers function (via the parameter r). One can easily see that $\mathcal{Q}(q_T)$ has a maximum when

$$q_T = q_T^M = \sqrt{(1+r)/(1-r)}/\beta, \quad (46)$$

where its value is $\mathcal{Q}(q_T^M) \equiv \mathcal{Q}_M = [2r/(1+r)]^{3/2}$. Notice that the position of the maximum depends on the parameter β , while \mathcal{Q}_M only depends on $r = \beta^2/\alpha^2$. In particular, when $r = 0.7$, $q_T^M \simeq 2.38/\beta$, and $\mathcal{Q}_M \simeq 0.75$.

In order to collect statistical significance, one could integrate the asymmetry over \mathbf{q}_T , but this would lead to a vanishing result, due to the $\cos \phi_{q_T}$ factor. However, one can think of integrating over ϕ_{q_T} in the range $[0, \pi/2]$ only, or alternatively of taking into account the change of sign in the different quadrants. In both ways, the ϕ_{q_T} integration gives an overall factor $\int d\phi |\cos \phi| / \int d\phi = 2/\pi$.

We can then consider the magnitude of the asymmetry averaged over \mathbf{q}_T up to an upper value of $q_T = q_{T1}$. In our simple model, Eq. (45), one obtains

$$\begin{aligned} \langle |A_N(M, y, \mathbf{q}_T)| \rangle_{q_{T1}} &= \frac{\int^{q_{T1}} d^2 \mathbf{q}_T |A_N(M, y, \mathbf{q}_T)| d\sigma}{\int^{q_{T1}} d^2 \mathbf{q}_T d\sigma} = \frac{\int^{q_{T1}} d^2 \mathbf{q}_T (d\sigma^\uparrow - d\sigma^\downarrow)}{\int^{q_{T1}} d^2 \mathbf{q}_T (d\sigma^\uparrow + d\sigma^\downarrow)} \\ &= \frac{1}{\pi} r^{3/2} \left(2e \frac{1-r}{1+r} \right)^{1/2} \left\{ \sqrt{\pi} \text{Erf}(w) - 2w e^{-w^2} \right\} \left(1 - e^{-(1+r)w^2/2} \right)^{-1} \mathcal{A}(M, y) \\ &= \tilde{\mathcal{Q}}(q_{T1}) \mathcal{A}(M, y) \end{aligned} \quad (47)$$

where $d\sigma$ stands for $d\sigma/dy dM^2 d^2 \mathbf{q}_T$, $w = \beta q_{T1}/\sqrt{1+r}$ and $\mathcal{A}(M, y)$ is given by the last line of Eq. (45). In particular, when $q_{T1} \rightarrow \infty$, one finds the very simple result:

$$\langle |A_N(M, y, \mathbf{q}_T)| \rangle_\infty = \left(\frac{2e}{\pi} \right)^{1/2} r^{3/2} \left(\frac{1-r}{1+r} \right)^{1/2} \mathcal{A}(M, y). \quad (48)$$

This expression holds with a good accuracy already at $q_{T1} \gtrsim 1/\beta$.

Notice again that, concerning the intrinsic motion dependence, the above average is independent of β and depends only on r , via a function which has a maximum at $r = (\sqrt{10} - 1)/3 \simeq 0.72$, very close to the value $r = 0.7$ adopted in our analysis.

In Figs. 2 to 5 we show our model estimates for the SSA, starting from Eq. (45). In Fig. 2 we plot A_N as a function of y : the asymmetry is averaged over M , in the two kinematical ranges $6 \leq M \leq 10$ GeV and $10 \leq M \leq 20$ GeV, corresponding to the solid and the dashed curve respectively. We have fixed $q_T = q_T^M$, Eq. (46), and $\phi_{q_T} = 0$, which maximizes the \mathbf{q}_T -dependent part of the asymmetry.

In Fig. 3 we show the same asymmetry, averaged over different rapidity ranges, $|y| \leq 2$ (solid curve) and $0 \leq y \leq 2$ (dashed curve).

We also show the dependence of A_N on x_F in Fig. 4 and on x_q in Fig. 5; these partonic variables ($x_F = x_q - x_{\bar{q}}$) are obviously related to y and M via Eq. (22). The integration over the non observed variables is done in such a way as to correspond to

the kinematical ranges $-2 \leq y \leq 2$, $6 \leq M \leq 10$ GeV (solid curve) and $-2 \leq y \leq 2$, $10 \leq M \leq 20$ GeV (dashed curve).

All asymmetries in Figs. 2-5 are evaluated at $q_T = q_T^M$: the value of the SSA at different q_T values may be obtained by simply rescaling the results of Figs. 2-5 by the factor $\mathcal{Q}(q_T)/\mathcal{Q}(q_T^M)$. This factor is plotted in Fig. 6. In order to show how its behaviour depends on the parameter β , we present results for $\beta = 1.25 (\text{GeV}/c)^{-1}$ and $\beta = 0.83 (\text{GeV}/c)^{-1}$.

Analogously, one can obtain the magnitude of the asymmetry averaged over \mathbf{q}_T , Eq. (47), by rescaling the values given in Figs. 2-5 by the appropriate factor: this factor is obtained by dividing $\tilde{\mathcal{Q}}(q_{T1})$, see Eq. (47), by $\mathcal{Q}(q_T^M)$, and it is shown in Fig. 7.

Our numerical estimates show that A_N can be well measurable within RHIC expected statistical accuracy. The actual values depend on the assumed functional form of the Siverson function and its role with valence quarks only. This reflects in the increase of A_N to sizeable values at large x_q , Fig. 5, and at large x_F , Fig. 4; in fact, x_F large and positive implies a large $x_q > x_F$.

4. Comments and conclusions

The single transverse spin phenomenology, within QCD dynamics and the factorization scheme, is a rich and interesting subject. It combines simple pQCD spin dynamics with new long distance properties of quark distribution and fragmentation; the experimental measurements are relatively easy and clear, many have been and many more will be performed in the near future, both at nucleon-nucleon and lepton-nucleon facilities.

Very recently a large single transverse spin asymmetry has been observed at RHIC, at the very first spin measurement at $\sqrt{s} = 200$ GeV, in $p^\uparrow p \rightarrow \pi X$ processes [35]; despite the large energy the asymmetry is not negligible, contrary to naive expectations.

The approach adopted here - and in many previous papers - requires the explicit control of parton intrinsic motion, which cannot be simply integrated over in the different non perturbative functions and the elementary dynamics, but must be kept into account wherever it can give new effects. Actually, this is true also for a correct computation of the unpolarized cross-sections, as it has been known for a long time, although somewhat forgotten. When dealing with spin dependences, the intrinsic motion is a rich and unexpected source of many new effects.

We have presented here the explicit formalism for computing single transverse spin asymmetries in Drell-Yan processes, within a generalized QCD factorization theorem formulated with \mathbf{k}_\perp dependent distribution functions. Simple gaussian forms have been assumed and available data from other processes have been exploited, in order to give estimates for single spin effects in D-Y production at RHIC, which should be of interest for the incoming measurements. Again, sizeable and measurable values have been found.

Our approach can and will be extended to the study of any $AB \rightarrow CX$ process, at large energy and moderate to large momentum transfer; the parton intrinsic motion is relevant both in polarized and unpolarized processes and the resulting phenomenology might explain or anticipate many subtle and unexpected results.

Acknowledgements

We would like to thank D. Boer for many useful discussions; U.D. and F.M. thank COFINANZIAMENTO MURST-PRIN for partial support.

References

- [1] For a review of data see, *e.g.*, K. Heller, in *Proceedings of Spin 96*, C.W. de Jager, T.J. Ketel and P. Mulders, Eds., World Scientific (1997); or A.D. Panagiotou, *Int. J. Mod. Phys. A* **5** (1990) 1197
- [2] D.L. Adams *et al.*, *Phys. Lett. B* **264** (1991) 462; A. Bravar *et al.*, *Phys. Rev. Lett.* **77** (1996) 2626
- [3] HERMES Collaboration, A. Airapetian *et al.*, *Phys. Rev. Lett.* **84** (2000) 4047; *Phys. Rev. D* **64** (2001) 097101
- [4] For review papers on the subject, see C. Boros and Liang Zuo-Tang, *Int. J. Mod. Phys. A* **15** (2000) 92; M. Anselmino, e-Print Archive: hep-ph/0201150
- [5] J.C. Collins, *Nucl. Phys. B* **396** (1993) 16
- [6] J.C. Collins, D.E. Soper and G. Sterman, *Nucl. Phys. B* **250** (1985) 199; J.C. Collins and D.E. Soper, *Nucl. Phys. B* **193** (1981) 381
- [7] R.D. Field and R.P. Feynman, *Phys. Rev. D* **15** (1977) 2590; R.P. Feynman, R.D. Field and G.C. Fox, *Phys. Rev. D* **18** (1978) 3320
- [8] X-N. Wang, *Phys. Rev. C* **61** (2000) 064910; C.-Y. Wong and H. Wang, *Phys. Rev. C* **58** (1998) 376; Y. Zhang, G. Fai, G. Papp, G. Barnaföldi and P. Lévai, *Phys. Rev. C* **65** (2002) 034903
- [9] M. Boglione and P.J. Mulders, *Phys. Rev. D* **60** (1999) 054007
- [10] D. Boer and P.J. Mulders, *Phys. Rev. D* **57** (1998) 5780
- [11] D. Boer, *Phys. Rev. D* **60** (1999) 014012
- [12] R. Jakob and P.J. Mulders, e-Print Archive: hep-ph/9610295
- [13] V. Barone, A. Drago and P. Ratcliffe, *Phys. Rep.* **359** (2002) 1
- [14] D. Sivers, *Phys. Rev. D* **41** (1990) 83; *Phys. Rev. D* **43** (1991) 261
- [15] M. Anselmino, M. Boglione and F. Murgia, *Phys. Lett. B* **362** (1995) 164; M. Anselmino and F. Murgia, *Phys. Lett. B* **442** (1998) 470
- [16] M. Anselmino, M. Boglione and F. Murgia, *Phys. Rev. D* **60** (1999) 054027
- [17] M. Boglione and E. Leader, *Phys. Rev. D* **61** (2000) 114001
- [18] M. Anselmino, D. Boer, U. D'Alesio and F. Murgia, *Phys. Rev. D* **63** (2001) 054029

- [19] M. Anselmino, V. Barone, A. Drago and F. Murgia, *Nucl. Phys. Proc. Suppl.* **105** (2002) 132; e-Print Archive: hep-ph/0209073
- [20] S.J. Brodsky, D.S. Hwang and I. Schmidt, *Phys. Lett.* **B530** (2002) 99
- [21] J.C. Collins, *Phys. Lett.* **B536** (2002) 43
- [22] X. Ji and F. Yuan, *Phys. Lett.* **B543** (2002) 66
- [23] S.J. Brodsky, D.S. Hwang and I. Schmidt, *Nucl. Phys.* **B642** (2002) 344
- [24] G. Bunce, N. Saito, J. Soffer and W. Vogelsang, *Ann. Rev. Nucl. Part. Sci.* **50** (2000) 525, e-Print Archive: hep-ph/0007218
- [25] N. Hammon, O. Teryaev and A. Schäfer, *Phys. Lett.* **B390** (1997) 409
- [26] D. Boer, P.J. Mulders and O. Teryaev, *Phys. Rev.* **D57** (1998) 3057
- [27] D. Boer and P.J. Mulders, *Nucl. Phys.* **B569** (2000) 505
- [28] D. Boer and J. Qiu, *Phys. Rev.* **D65** (2002) 034008
- [29] J. Qiu and G. Sterman, *Phys. Rev. Lett.* **67** (1991) 2264; *Nucl. Phys.* **B378** (1992) 52; *Nucl. Phys.* **B353** (1991) 105; *Nucl. Phys.* **B353** (1991) 137
- [30] J.C. Collins and D.E. Soper, *Phys. Rev.* **D16** (1977) 2219
- [31] C. Boros, Liang Zuo-Tang and Meng Ta-chung, *Phys. Rev. Lett.* **70** (1993) 1751; C. Boros and Meng Ta-chung, *Phys. Rev.* **D52** (1995) 529
- [32] M. Anselmino, D. Boer, U. D'Alesio and F. Murgia, *Phys. Rev.* **D65** (2002) 114014
- [33] M. Gluck, E. Reya, A. Vogt, *Z. Phys.* **C67** (1995) 433
- [34] U. D'Alesio and F. Murgia, work in preparation; see also the talk by U. D'Alesio at SPIN 2002, Brookhaven National Laboratory, September 9-14, 2002, to appear in the proceedings.
- [35] See the talk by G. Rakness at SPIN 2002, Brookhaven National Laboratory, September 9-14, 2002, to appear in the proceedings.

Figure captions

Fig. 1: The kinematical configuration considered in this paper. The γ^* four-momentum defines all our observables; the dependence on the angle between the γ^* - z and the γ^* -($\ell^+\ell^-$) planes is integrated over in Eq.s (12) and (14).

Fig. 2: The single spin asymmetry A_N for the Drell-Yan process, see Eq. (45), at RHIC energies, $\sqrt{s} = 200$ GeV, as a function of the rapidity y and averaged over the invariant mass ranges $6 \leq M \leq 10$ GeV (solid line) and $10 \leq M \leq 20$ GeV (dashed line). Results are given at $q_T = q_T^M$, see Eq. (46), and $\phi_{q_T} = 0$, which maximizes the effect. Furthermore, we have used $r = 0.7$, the parameters of Eq. (42) for the Siverson function (see text for further details) and the parameterization GRV94 [33] for the unpolarized parton distributions. Notice that the asymmetry is practically negligible in the range $y < 0$.

Fig. 3: The single spin asymmetry A_N for the Drell-Yan process, see Eq. (45), at RHIC energies, $\sqrt{s} = 200$ GeV, as a function of the invariant mass M and averaged over the rapidity ranges $-2 \leq y \leq 2$ (solid line) and $0 \leq y \leq 2$ (dashed line). Results are given at $q_T = q_T^M$, see Eq. (46), and $\phi_{q_T} = 0$, which maximizes the effect. Furthermore, we have used $r = 0.7$, the parameters of Eq. (42) for the Siverson function (see text for further details) and the parameterization GRV94 [33] for the unpolarized parton distributions.

Fig. 4: The single spin asymmetry A_N for the Drell-Yan process, see Eq. (45), at RHIC energies, $\sqrt{s} = 200$ GeV, as a function of the Feynman variable $x_F = x_q - x_{\bar{q}}$ and averaged over the rapidity and the invariant mass in the ranges $-2 \leq y \leq 2$, $6 \leq M \leq 10$ GeV (solid line) and $-2 \leq y \leq 2$, $10 \leq M \leq 20$ GeV (dashed line). Results are given at $q_T = q_T^M$, see Eq. (46), and $\phi_{q_T} = 0$, which maximizes the effect. Furthermore, we have used $r = 0.7$, the parameters of Eq. (42) for the Siverson function (see text for further details) and the parameterization GRV94 [33] for the unpolarized parton distributions. The two curves almost coincide but the solid line, corresponding to a lower invariant mass range, cannot reach values of $x_F \gtrsim 0.36$ within the given y range. Notice that the asymmetry is practically negligible in the range $x_F < 0$.

Fig. 5: The single spin asymmetry A_N for the Drell-Yan process, see Eq. (45), at RHIC energies, $\sqrt{s} = 200$ GeV, as a function of x_q and averaged over the rapidity and the invariant mass in the ranges $-2 \leq y \leq 2$, $6 \leq M \leq 10$ GeV (solid line) and $-2 \leq y \leq 2$, $10 \leq M \leq 20$ GeV (dashed line). Results are given at $q_T = q_T^M$, see Eq. (46), and $\phi_{q_T} = 0$, which maximizes the effect. Furthermore, we have used $r = 0.7$, the parameters of Eq. (42) for the Siverson function (see text for further details) and the parameterization GRV94 [33] for the unpolarized parton distributions. The two curves almost coincide but the solid line, corresponding to a lower invariant mass range, cannot reach values of $x_q \gtrsim 0.37$ within the given y range.

Fig. 6: The factor $\mathcal{Q}(q_T)/\mathcal{Q}(q_T^M)$, see Eq.s (45) and (46), plotted as a function of q_T , for $\beta = 1.25 \text{ (GeV/c)}^{-1}$ (solid line) and $\beta = 0.83 \text{ (GeV/c)}^{-1}$ (dashed line), corresponding respectively to $\langle k_\perp^2 \rangle^{1/2} = 0.8 \text{ GeV/c}$ and $\langle k_\perp^2 \rangle^{1/2} = 1.2 \text{ GeV/c}$. This factor can be used to rescale the asymmetries given in Fig.s 2-5, at $q_T = q_T^M$, to their values at q_T different from q_T^M .

Fig. 7: The factor $\tilde{\mathcal{Q}}(q_{T1})/\mathcal{Q}(q_T^M)$, see Eq.s (47) and (46), plotted as a function of q_{T1} , for $\beta = 1.25 \text{ (GeV/c)}^{-1}$ (solid line) and $\beta = 0.83 \text{ (GeV/c)}^{-1}$ (dashed line), corresponding respectively to $\langle k_\perp^2 \rangle^{1/2} = 0.8 \text{ GeV/c}$ and $\langle k_\perp^2 \rangle^{1/2} = 1.2 \text{ GeV/c}$. This factor can be used to obtain from the asymmetries given in Fig.s 2-5 (at fixed \mathbf{q}_T , $q_T = q_T^M$ and $\phi_{q_T} = 0$) the corresponding asymmetries averaged over \mathbf{q}_T up to $|\mathbf{q}_T| = q_{T1}$ (see text for further details).

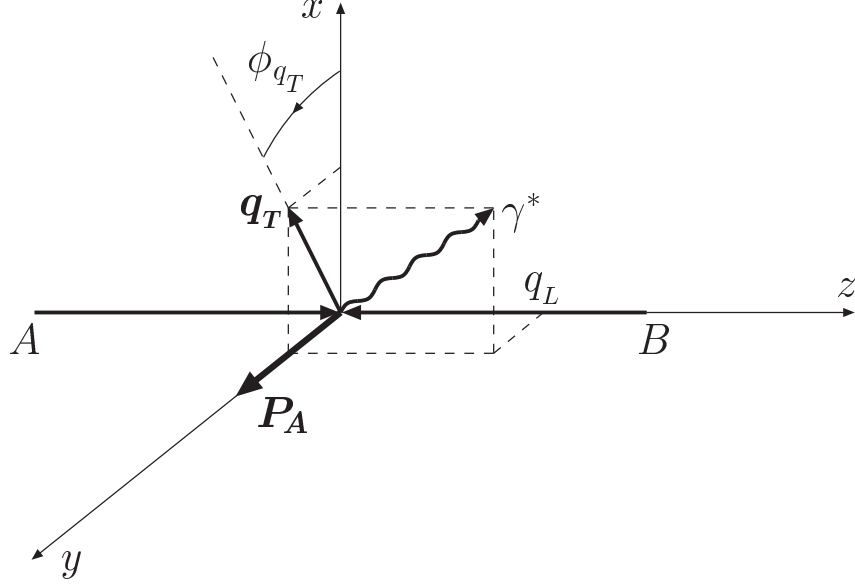


Figure 1: The kinematical configuration considered in this paper. The γ^* four-momentum defines all our observables; the dependence on the angle between the γ^* - z and the γ^* -($\ell^+\ell^-$) planes is integrated over in Eq.s (12) and (14).

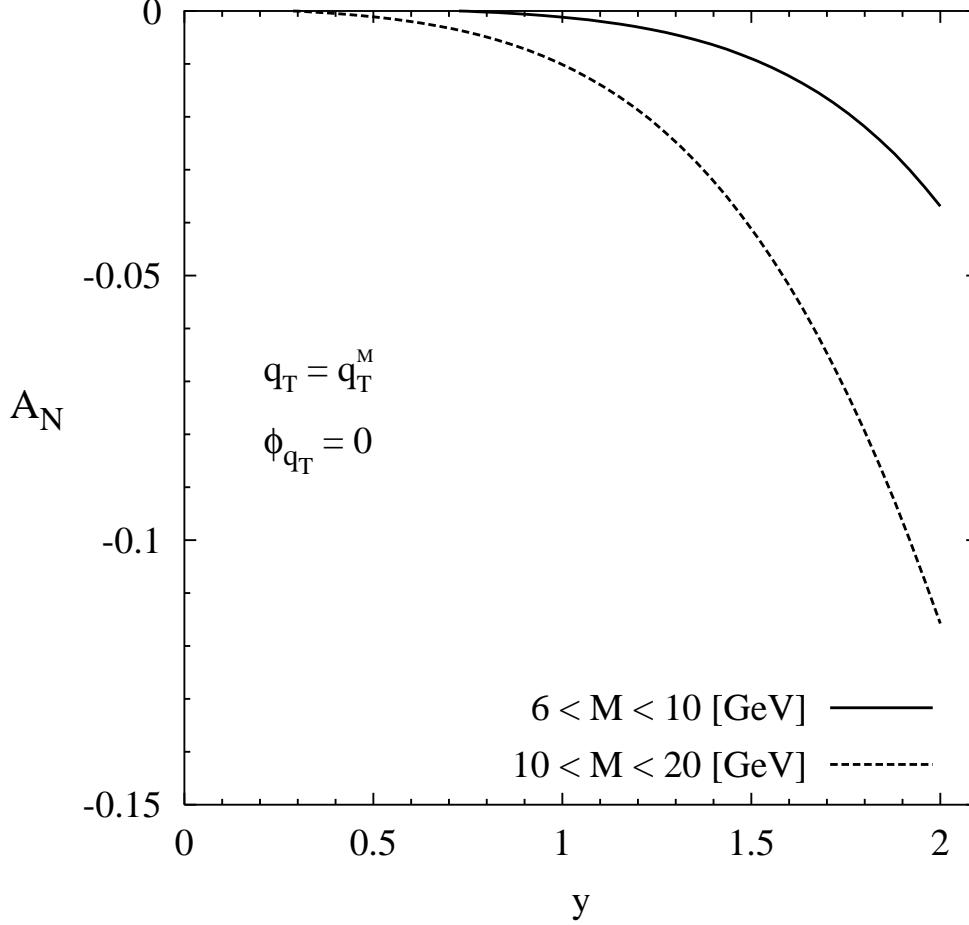


Figure 2: The single spin asymmetry A_N for the Drell-Yan process, see Eq. (45), at RHIC energies, $\sqrt{s} = 200$ GeV, as a function of the rapidity y and averaged over the invariant mass ranges $6 \leq M \leq 10$ GeV (solid line) and $10 \leq M \leq 20$ GeV (dashed line). Results are given at $q_T = q_T^M$, see Eq. (46), and $\phi_{q_T} = 0$, which maximizes the effect. Furthermore, we have used $r = 0.7$, the parameters of Eq. (42) for the Siverson function (see text for further details) and the parameterization GRV94 [33] for the unpolarized parton distributions. Notice that the asymmetry is practically negligible in the range $y < 0$.

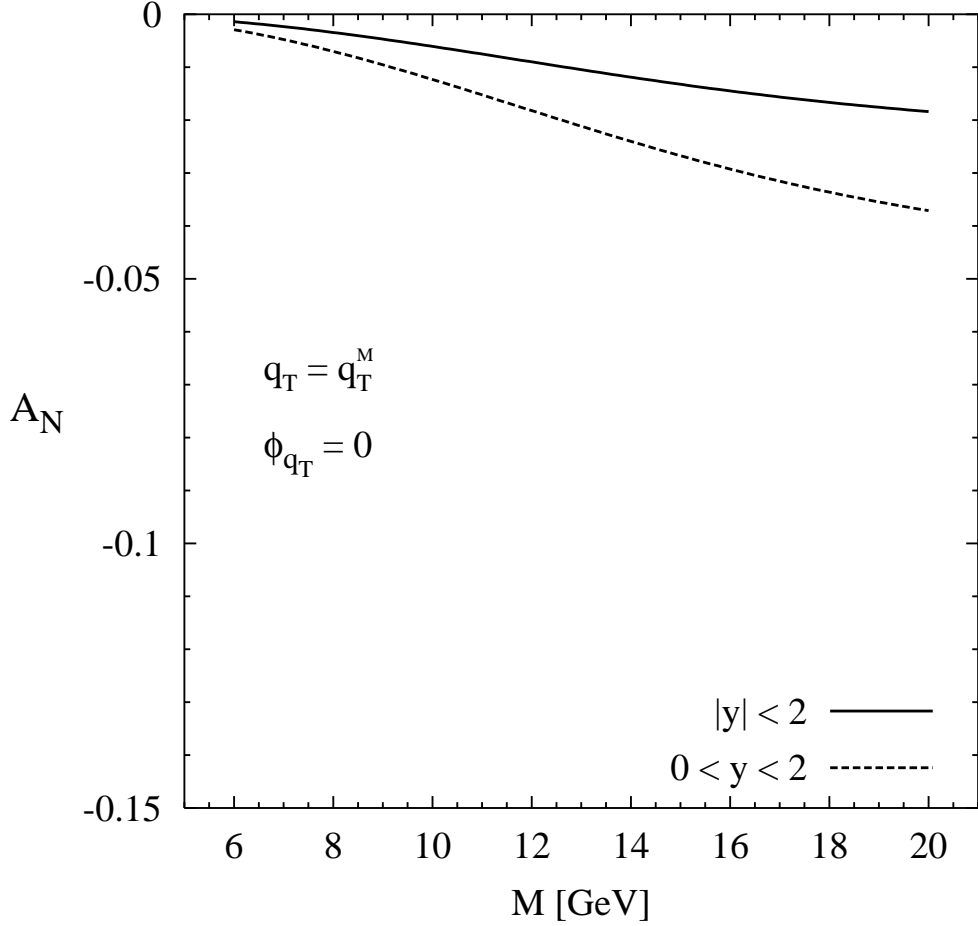


Figure 3: The single spin asymmetry A_N for the Drell-Yan process, see Eq. (45), at RHIC energies, $\sqrt{s} = 200$ GeV, as a function of the invariant mass M and averaged over the rapidity ranges $-2 \leq y \leq 2$ (solid line) and $0 \leq y \leq 2$ (dashed line). Results are given at $q_T = q_T^M$, see Eq. (46), and $\phi_{q_T} = 0$, which maximizes the effect. Furthermore, we have used $r = 0.7$, the parameters of Eq. (42) for the Sivers function (see text for further details) and the parameterization GRV94 [33] for the unpolarized parton distributions.

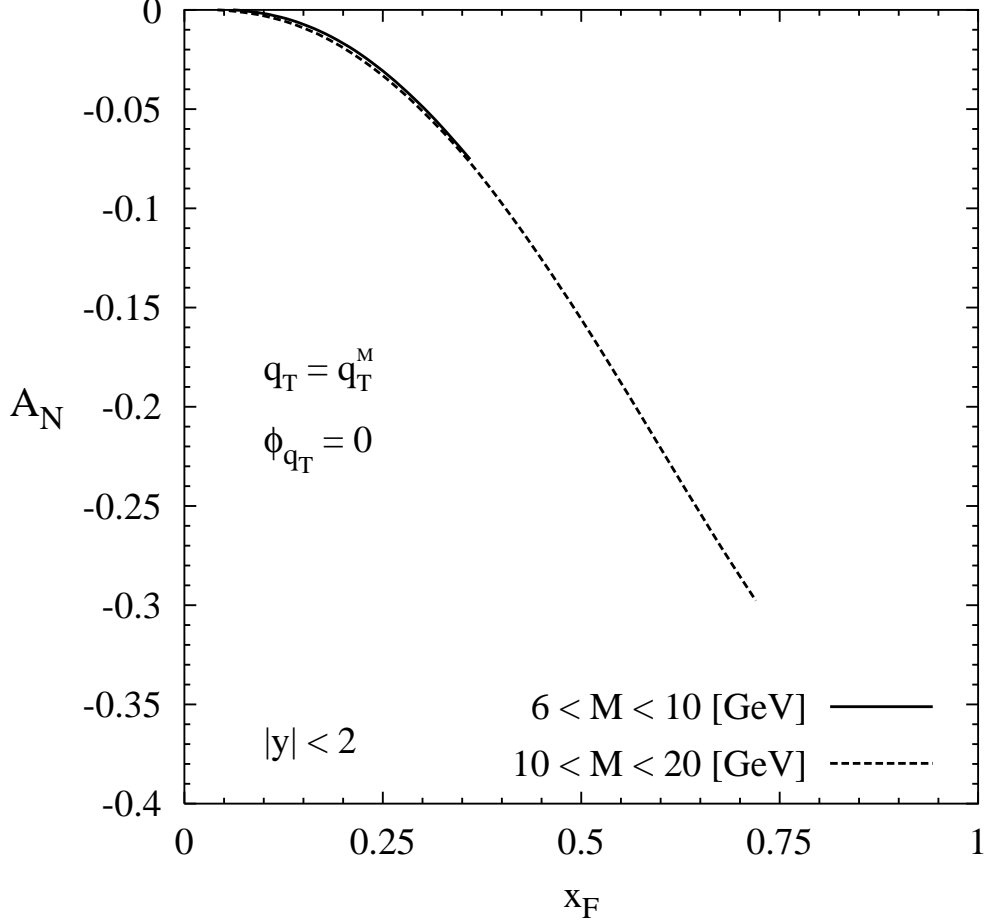


Figure 4: The single spin asymmetry A_N for the Drell-Yan process, see Eq. (45), at RHIC energies, $\sqrt{s} = 200$ GeV, as a function of the Feynman variable $x_F = x_q - x_{\bar{q}}$ and averaged over the rapidity and the invariant mass in the ranges $-2 \leq y \leq 2$, $6 \leq M \leq 10$ GeV (solid line) and $-2 \leq y \leq 2$, $10 \leq M \leq 20$ GeV (dashed line). Results are given at $q_T = q_T^M$, see Eq. (46), and $\phi_{q_T} = 0$, which maximizes the effect. Furthermore, we have used $r = 0.7$, the parameters of Eq. (42) for the Siverson function (see text for further details) and the parameterization GRV94 [33] for the unpolarized parton distributions. The two curves almost coincide but the solid line, corresponding to a lower invariant mass range, cannot reach values of $x_F \gtrsim 0.36$ within the given y range. Notice that the asymmetry is practically negligible in the range $x_F < 0$.

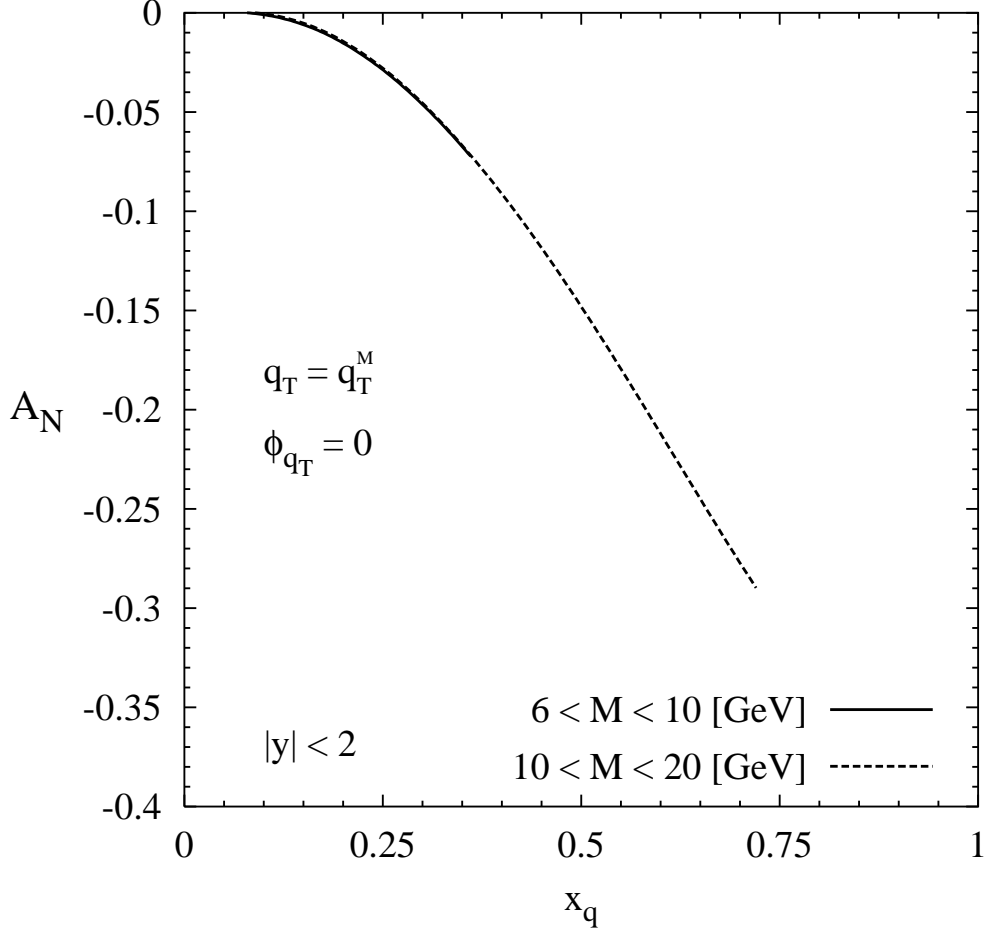


Figure 5: The single spin asymmetry A_N for the Drell-Yan process, see Eq. (45), at RHIC energies, $\sqrt{s} = 200$ GeV, as a function of x_q and averaged over the rapidity and the invariant mass in the ranges $-2 \leq y \leq 2$, $6 \leq M \leq 10$ GeV (solid line) and $-2 \leq y \leq 2$, $10 \leq M \leq 20$ GeV (dashed line). Results are given at $q_T = q_T^M$, see Eq. (46), and $\phi_{q_T} = 0$, which maximizes the effect. Furthermore, we have used $r = 0.7$, the parameters of Eq. (42) for the Sivers function (see text for further details) and the parameterization GRV94 [33] for the unpolarized parton distributions. The two curves almost coincide but the solid line, corresponding to a lower invariant mass range, cannot reach values of $x_q \gtrsim 0.37$ within the given y range.

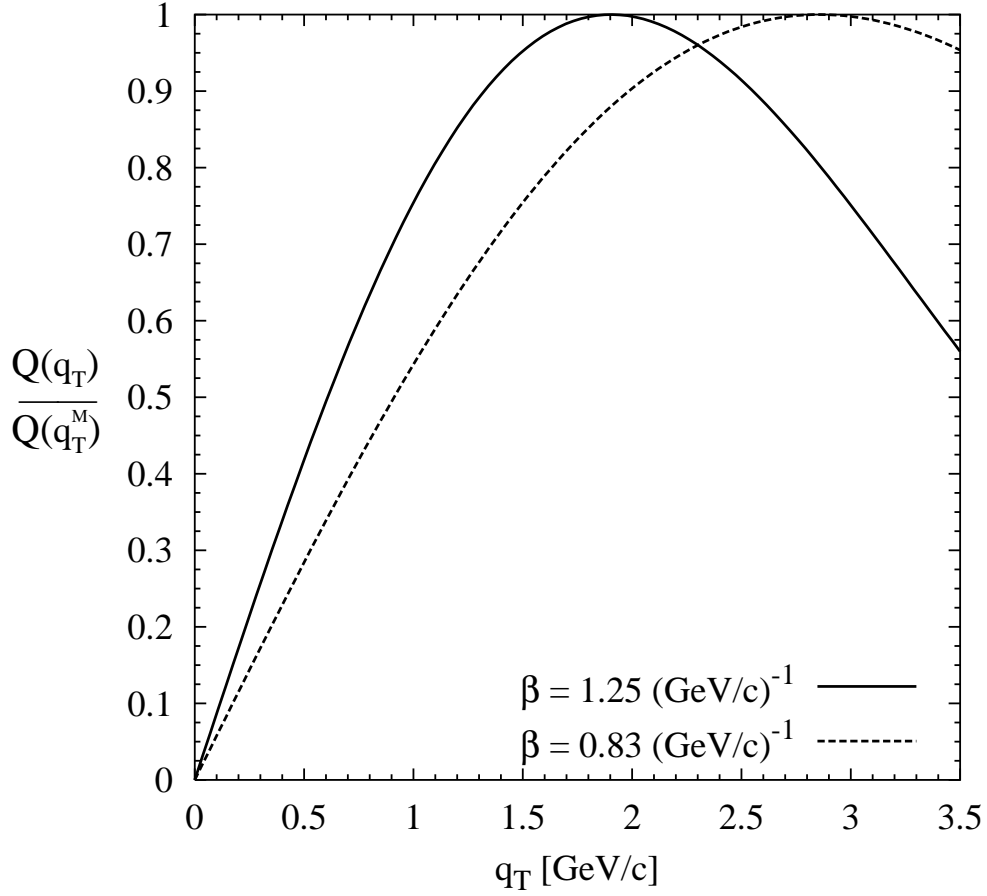


Figure 6: The factor $\mathcal{Q}(q_T)/\mathcal{Q}(q_T^M)$, see Eq.s (45) and (46), plotted as a function of q_T , for $\beta = 1.25 \text{ (GeV/c)}^{-1}$ (solid line) and $\beta = 0.83 \text{ (GeV/c)}^{-1}$ (dashed line), corresponding respectively to $\langle k_\perp^2 \rangle^{1/2} = 0.8 \text{ GeV/c}$ and $\langle k_\perp^2 \rangle^{1/2} = 1.2 \text{ GeV/c}$. This factor can be used to rescale the asymmetries given in Figs 2-5, at $q_T = q_T^M$, to their values at q_T different from q_T^M .

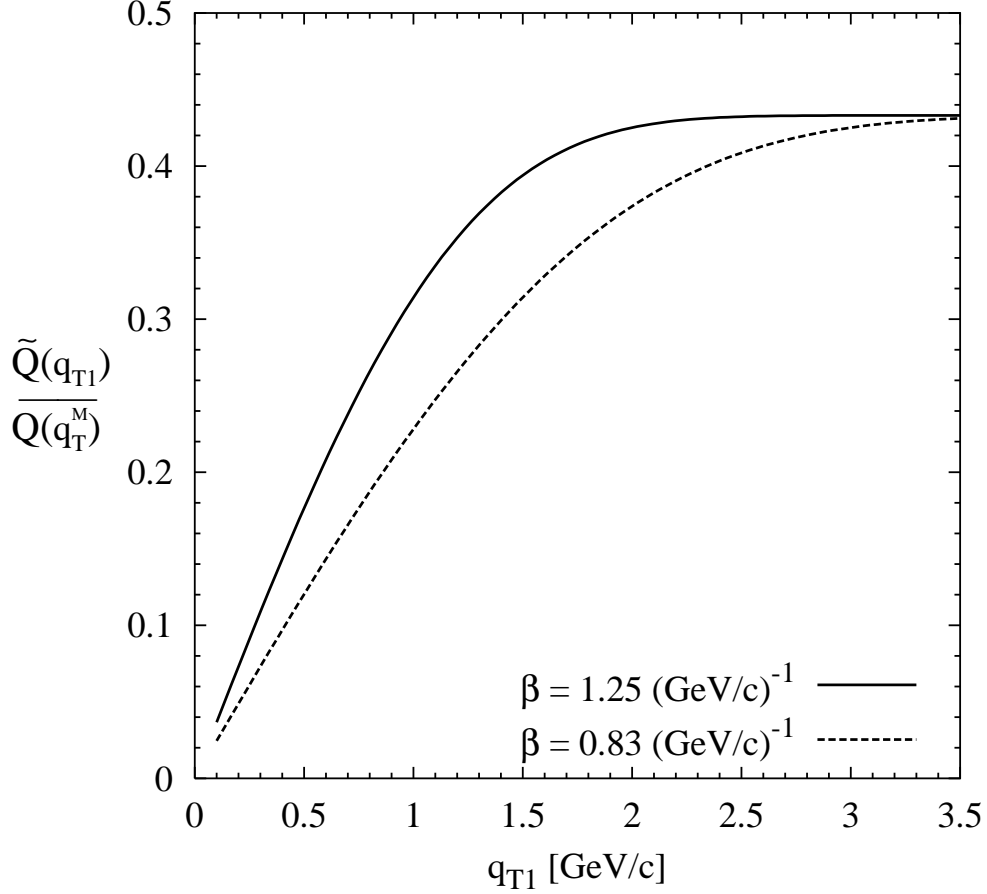


Figure 7: The factor $\tilde{Q}(q_{T1})/\overline{Q}(q_T^M)$, see Eq.s (47) and (46), plotted as a function of q_{T1} , for $\beta = 1.25 \text{ (GeV/c)}^{-1}$ (solid line) and $\beta = 0.83 \text{ (GeV/c)}^{-1}$ (dashed line), corresponding respectively to $\langle k_{\perp}^2 \rangle^{1/2} = 0.8 \text{ GeV/c}$ and $\langle k_{\perp}^2 \rangle^{1/2} = 1.2 \text{ GeV/c}$. This factor can be used to obtain from the asymmetries given in Figs 2-5 (at fixed \mathbf{q}_T , $q_T = q_T^M$ and $\phi_{q_T} = 0$) the corresponding asymmetries averaged over \mathbf{q}_T up to $|\mathbf{q}_T| = q_{T1}$ (see text for further details).